

Supporting Information

Two-dimensional Kagome Lattices Made of Hetero Triangulenes are Dirac Semimetals or Single-Band Semiconductors

Yu Jing^{1,2}, Thomas Heine^{1,2,3,*}

- 1 Wilhelm-Ostwald-Institut für Physikalische und Theoretische Chemie, Linnéstr.
2, 04103 Leipzig, Germany;
- 2 TU Dresden, Fakultät Chemie und Lebensmittelchemie, Bergstraße 66c, 01062
Dresden, Germany.
- 3 Helmholtz-Zentrum Dresden-Rossendorf, Forschungsstelle Leipzig,
Permoserstraße 15, 04318 Leipzig, Germany

*Correspondence and requests for materials should be addressed to T. H. (email:
thomas.heine@tu-dresden.de

Computational methods

Methods

The structures of HT(N/B)s were optimized by using Amsterdam Density Functional (ADF) package.¹

The lattices of **kgm** polymers were optimized by employing first-principles calculations on basis of density functional theory (DFT), as implemented in Vienna *ab initio* simulation package (VASP). An efficient memory conserving symmetrization of the charge density is used. Projector-augmented plane wave (PAW) approach was employed to describe the ion–electron interactions. All calculations have first been carried out using the PBE functional, and electronic structures have been refined by the Herd–Scuseria–Ernzerhof hybrid functional (HSE06). All the examined 2D **kgm** structures have a diamagnetic ground state. For more details on method validation, structural stability, electronic calculations, please see SI.

For the closed shell hetero-triangulenes (HT(N/B)s) systems, spin restricted all electron calculations were performed with the TZP basis set and good numerical quality at the B3LYP levels of theory.

For calculations of Kagome (**kgm**) polymers, a convergence threshold of 10^{-4} eV in energy and 10^{-2} eV Å⁻¹ for the force within the conjugated gradient method for geometry optimizations and a cutoff energy of 450 eV for the plane-wave basis set were adopted in all computations. Our results have been validated for band gap and density-of-states of **kgm**

CTPA, which have been experimentally determined by scanning tunneling spectroscopy (2.45 ± 0.09 eV), and are in excellent agreement with our HSE06 calculations (2.46 eV for **kgm** CTPA). The k-point mesh of the Brillouin zone was set to be $5 \times 5 \times 1$ for geometry optimization and calculations of electronic structure. Although our DFT calculations neglect the exciton binding energy, the HSE06 functional is known to produce band gaps close to experiment for similar organic semiconductors.^{2,3} The spin-orbital coupling (SOC) effect was considered when we examined the band structure of **kgm** HT(C)-polymers. No appreciable difference was observed for the band structures calculated with and without SOC effect at the PBE level. Therefore, the **kgm** HT(C)-polymers turn out to be semimetals instead of topological semiconductors and the SOC effect is not considered in the presented results.

The reaction energy (E_r) of **kgm** HT(N/B)-polymers is calculated to estimate the feasibility of synthesizing these systems from hetero-triangulene monomers, which is according to equation:

$$E_r = [E_{\text{polymer}} - (2E_{\text{monomer}} - 3E_{\text{H}_2})]/n_{\text{polymer}} \quad (\text{S1})$$

where E_{polymer} and n_{polymer} represent the total energy and total atom number of **kgm** HT(N/B)-polymers, E_{monomer} and E_{H_2} represent the total energy of the molecular monomer and hydrogen in the gas phase, respectively. Phonon spectra were computed by using the finite displacement approach as implemented in the phonopy code on basis of density functional perturbation theory.^{4,5} The thermodynamic stability of **kgm** HT(N/B)-polymers were accessed by performing Born-Oppenheimer molecular dynamic (BOMD) simulations at 500 K by using VASP. The time step is 1 fs and the total simulation time is 5 ps.

In non-polar semiconductors, the electron is mainly scattered by acoustic phonon and the intrinsic mobility caused by acoustic phonon scattering can be described by the deformation potential (DP) theory,⁶ which has turned out to be reliable in predicting the carrier mobilities of inorganic and organic monolayers like MoS₂, phosphorene and graphdiyne sheets.⁷⁻⁹ According to the deformation theory, the carrier mobility of **kgm** HT(N/B)-polymers can be examined via equation¹⁰

$$\mu_{2D} = \frac{2e\hbar^3 C_{2D}}{3k_B T |m^*|^2 E_1^2} \quad (\text{S2})$$

where \hbar is the reduced Planck constant, k_B is Boltzmann constant, and T is the temperature (set to be 300 K). The carrier mobilities of **kgm** HT(N/B)-polymers can be accessed by Equation S2 after the effective masses m^* , in-plane stiffness C_{2D} and deformation potential E_1 are known.

D_{3h} (HT)₆-oligomer resemble to benzene

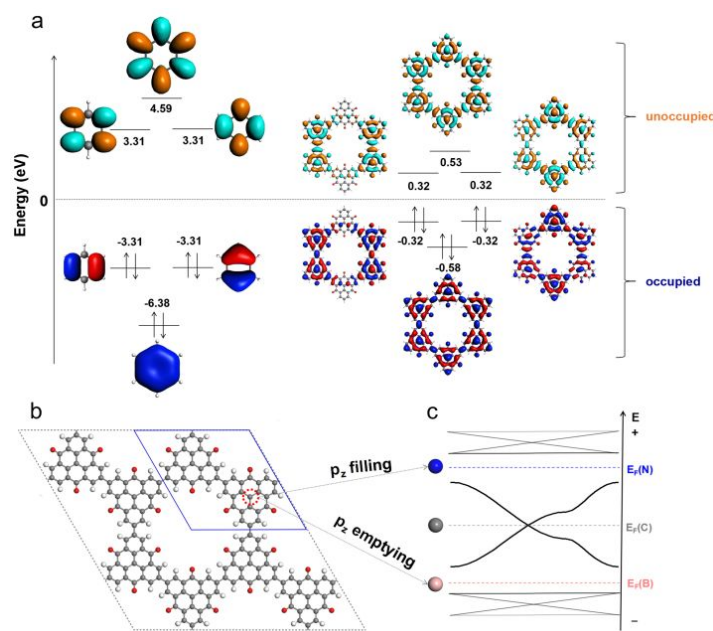


Figure S1.(a) Frontier molecular orbitals and schematics of energy levels for D_{3h} carbonyl-bridged triphenylmethyl radical (CTP) oligomer (D_{3h} (CTP)6) in comparison with those of benzene. The dashed line represents the isolated p orbitals and is set to be 0 eV. (b) a kgm CTP-polymer structure in a 2×2×1 supercell, the blue line indicates the unit cell; (c) centre-atom dependent band structure. EF(N), EF(C) and EF(B) denote the positions of the Fermi levels of corresponding kgm HT(N/C/B)-polymers.

Geometry and stability of **kgm** HT-polymers

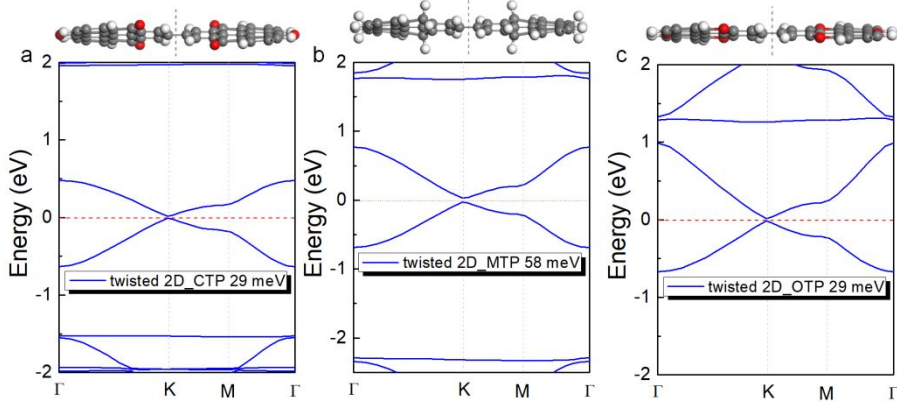


Figure S2. Band gap opening of twisted **kgm** HT(C)-polymers. (a-c), schematics and band structure of CTP, MTP and OTP based **kgm** polymers that calculated at the HSE06 functional of theory. The value of the opened band gap is shown within the band structures.

Table S1. Lattice parameters (L), pore size (P), distance of two in-plane neighbouring centre atoms (D) and reaction energy (E_r) per unit of optimized planar **kgm** HT polymers. The HT(B)-polymers always show somewhat larger lattice constants and pore sizes than their N centred counterparts.

kgm polymers	CTPB	CTP	CTPA	MTPB	MTP	MTPA	OTPB	OTP	OTPA
L /Å	17.58	17.40	17.36	17.62	17.47	17.42	17.17	17.09	17.07
P /Å	11.98	11.78	11.75	13.10	12.92	12.90	12.80	12.72	12.71
D /Å	10.15	10.05	10.02	10.17	10.09	10.06	9.91	9.87	9.86
E_r /eV	1.63	—	1.74	1.54	—	1.36	1.86	—	1.49

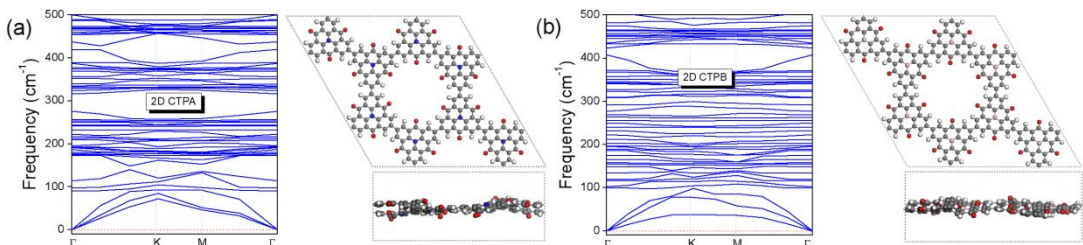


Figure S3. Phonon spectra and structure after a 5ps BOMD simulation at 500K for (a) **kgm** CTPA and (b) CTPB. The highest-energy phonons (corresponding to C=O and C-H vibrations) reach to ~ 3160 cm^{-1} . We show here only the range up to 500 cm^{-1} to give a clear picture that the phonon dispersions contain only real frequencies. The structures remain intact at 500K after a 5ps BOMD simulation. Similar results were also found for other **kgm**

HT(N/B) polymers. This confirms that these single-band semiconductors of **kgm** HT(N/B)-polymers are dynamically and thermodynamically stable.

Comparison between twisted and planar **kgm** HT(N/B)-polymers

Table S2. Lattice parameters (L) and pore size (P) of twisted **kgm** HT(N/B)-polymers, and the total energy difference (ΔE_{total}) between flat and twisted structures, $\Delta E_{\text{total}} = E_{\text{planar}} - E_{\text{twisted}}$, the band gaps (E_{band}) as well as the effective masses m^* (m_0 represents the electron rest mass) calculated at the PBE level. Structure distortion results in the lattice shrinkage and pore size decreasing. The twisted structures have lower energy than the flat ones, and the energy difference is in range of 0.03~0.15 eV. Therefore, structural distortion could happen if the 2D HT-polymers were isolated from the substrate or synthesized without a substrate.

kgm polymers	MTPB	MTPA	CTPB	CTPA	OTPB	OTPA
$L_{\text{twisted}} / \text{\AA}$	17.48	17.27	17.49	17.31	17.09	16.88
$P_{\text{twisted}} / \text{\AA}$	12.60	12.35	11.86	11.67	12.77	12.56
$\Delta E_{\text{total}} / \text{eV}$	0.15	0.10	0.04	0.03	0.12	0.04
$E_{\text{band}} / \text{eV}$	2.22	1.80	1.32	1.77	2.18	1.41
m^* / m_0	e_-0.47	h_-0.49	e_-0.35	h_-0.35	e_-0.38	h_-0.38

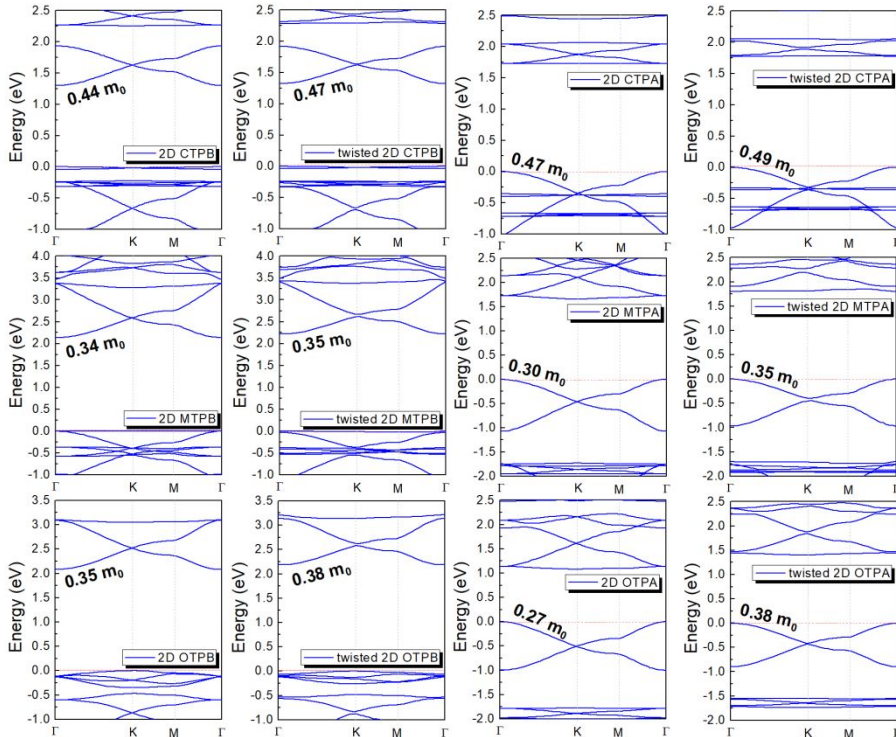


Figure S4. Band structures of twisted **kgm** HT(N/B)-polymers in comparison with those of the planar ones at the PBE level of theory. The Fermi level is set at the VBM and effective

masses for the dispersive band are indicated. The structure distortion has negligible effect on the band structure. The band gaps of twisted **kgm** HT(N/B)-polymers were calculated to be 2.22, 1.80, 1.32, 1.77, 2.18 and 1.41 eV for **kgm** MTPB-, MTPA-, CTPB-, CTPA-, OTPB- and OTPA-polymers, respectively. The values are slightly larger than those of the planar structures, which are 2.14, 1.66, 1.29, 1.73, 2.08, 1.08 eV respectively, at the same PBE level. This can be expected as the structures distortion will contribute to the decreasing of electron conjugation.

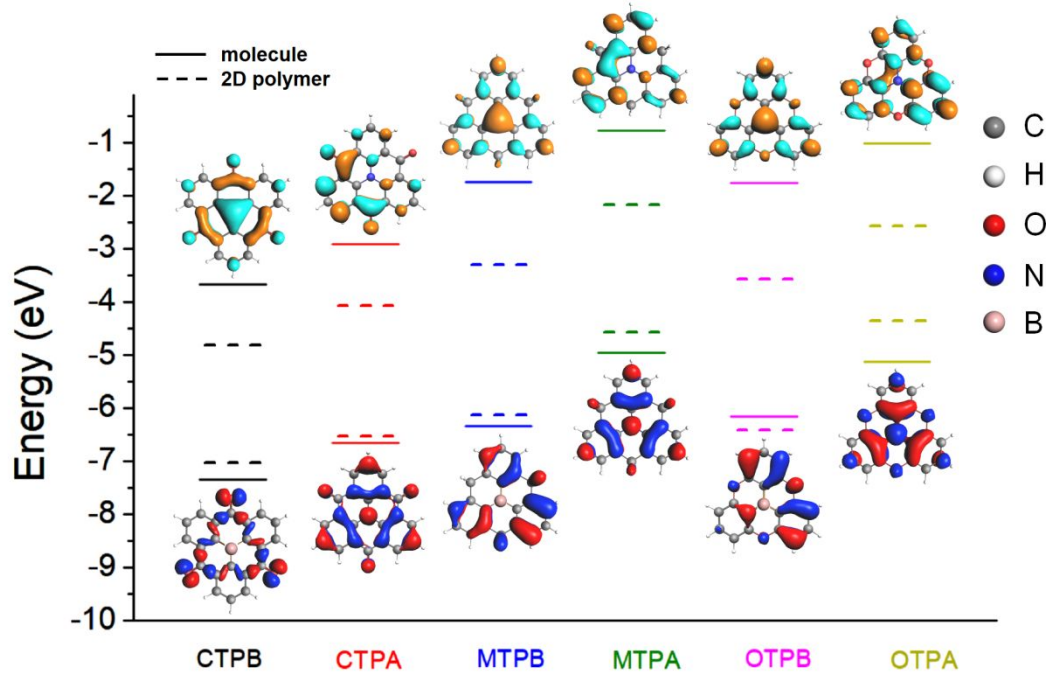


Figure S5. Band gap decreasing from HT(N/B) molecules to **kgm** HT(N/B)-polymers. Frontier orbital and band position of HT(N/B) molecules and corresponding **kgm** polymers. Functionalization of the bridge controls the π conjugation and thus the HOMO-LUMO gap of the HT molecules (it decreases from CH_2 via O to CO bridges both for B- and N-HTs), and consequently the band gap of the **kgm** HT(N/B)-polymers, which is smaller due to π conjugation and dispersion of the frontier band.

Carrier mobility of **kgm** HT(N/B)-polymers

Table S3. HSE06 vs. PBE. Effective masses for electrons (m_e^*) and holes (m_h^*) in **kgm** HT(N/B)-polymers that calculated by PBE and HSE06 methods. Although the band gap was underestimated by PBE functional, the predicted band structures and effective masses of the dispersive band were identical to the HSE06 results. Therefore, we further calculate the carrier mobilities of all single-band **kgm** HT(N/B)-polymers at the PBE level of theory.

kgm HT(N/B)-polymers	CTPB	CTPA	MTPB	MTPA	OTPB	OTPA
carrier	e	h	e	h	e	h
PBE / m_0	0.44	0.47	0.34	0.30	0.35	0.27
HSE06 / m_0	0.44	0.50	0.38	0.38	0.38	0.32

As shown in **Figure 2, S4** and **Tables S3**, PBE and HSE06 give very similar results except for the fact that PBE underestimates the band gap of the **kgm** HT(N/B) polymers.

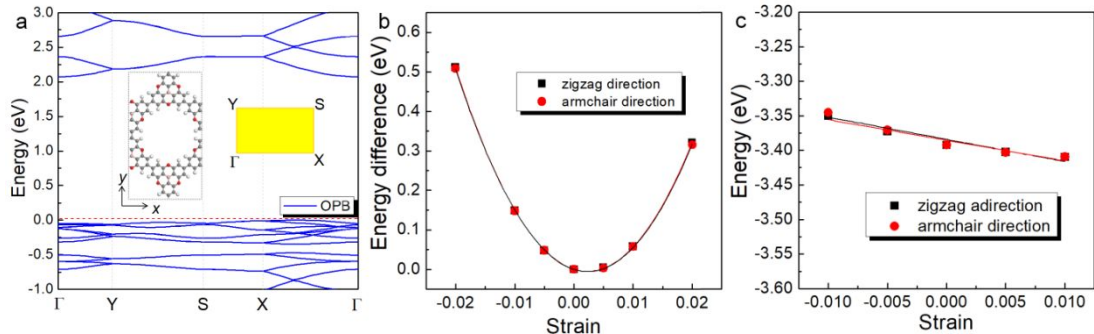


Figure S6. Simulations for carrier mobilities. (a) band structure of **kgm** CTPB-polymer in a rectangular supercell and the corresponding first Brillouin zone. (b) total energy difference between the equilibrium and diluted **kgm** CTPB-polymer as a function of the deformation along zigzag and armchair directions. The in-plane stiffness C_{2D} of **kgm** HT(N/B)-polymers, which is defined as $[\partial^2 E / \partial \delta^2] / S_0$, can be obtained by simulating the total energy (E) change with the variation of external uniaxial strain (δ) (S_0 is the area of the optimized supercell). (c) the CBM shift of **kgm** CTPB-polymer with the variation of deformation along different directions.

Table S4. Predicted Carrier mobility along armchair direction. Calculated effective masses m^* for electrons or holes, DP constant E_1 , in-plane stiffness C_{2D} and carrier mobility μ for **kgm** HT(N/B)-polymers along the armchair direction at the PBE level of theory. All 2D HT(B)-polymers show isotropic small m_e^* along zigzag and armchair directions, which are 0.44, 0.34, 0.35 m_0 for CTPB-, MTPB- and OTPB-polymers, respectively. In contrast, **kgm** HT(N)-polymers possess isotropic and small m_h^* of 0.30, 0.47 and 0.27 m_0 for CTPA-, MTPA- and OTPA-polymers, respectively. All **kgm** HT-polymer structures show nearly same effective masses along the zigzag and armchair directions, which indicates the highly isotropic electronic properties of the studied **kgm** HT-polymers systems. All structures show identical C_{2D} for the zigzag and armchair directions and the values are around 60 Nm^{-1} , which indicates isotropic mechanical properties of the studied **kgm** HT(N/B)-polymers. Via simulating the linear relation between the band edge energy (E_{edge}) and the strain exerted to the zigzag and armchair directions, we obtained the DP constant E_1 ($= \partial E_{\text{edge}} / \partial \delta$), which are also independent of the directions. As a result, the studied **kgm** HT(N/B)-polymers exhibit isotropic carrier mobility along zigzag and armchair directions, and B- and N-centered polymers show selectively high carrier mobilities for electrons and holes, respectively.

kgm HT(N/B)-polymers	CTPB	CTPA	MTPB	MTPA	OTPB	OTPA
Carrier	<i>e</i>	<i>h</i>	<i>e</i>	<i>h</i>	<i>e</i>	<i>h</i>
m^* / m_0	0.44	0.47	0.41	0.28	0.36	0.25
E_1 / eV	0.72	2.39	2.04	3.67	3.21	4.77
C_{2D} / Nm^{-1}	59.92	62.93	59.77	62.03	64.37	64.65
$\mu / \times 10^3 \text{ cm}^2 \text{V}^{-1} \text{s}^{-1}$	8.48	0.71	1.21	0.83	0.68	0.64

Orbitals of the flat bands in B, C and N centre 2D kgm polymers

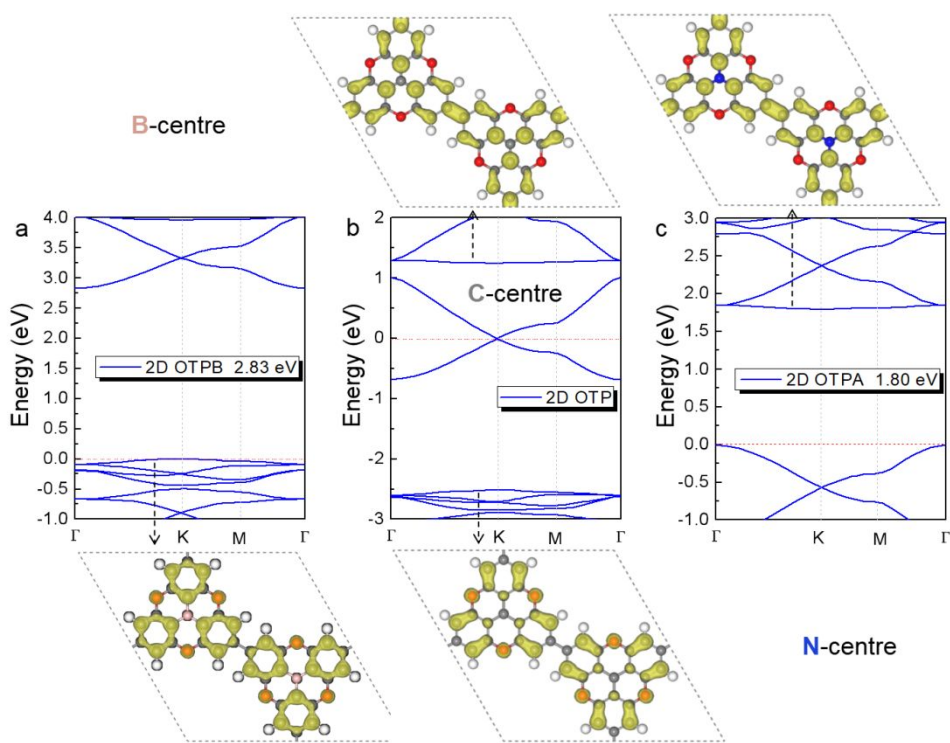


Figure S7. Orbitals of the flat bands in 2D OTPB (a), OTP (b) and OTPA (c), respectively. The isosurface of the flat band orbitals is set to be $0.001 \text{ e}\text{\AA}^{-3}$. It can be found that all the flat bands show no contribution of the centre atoms, independent of B, C or N, but are contributed by the delocalized orbitals of the reminder atoms.

PDOS of kgm HT(N/B)-polymers

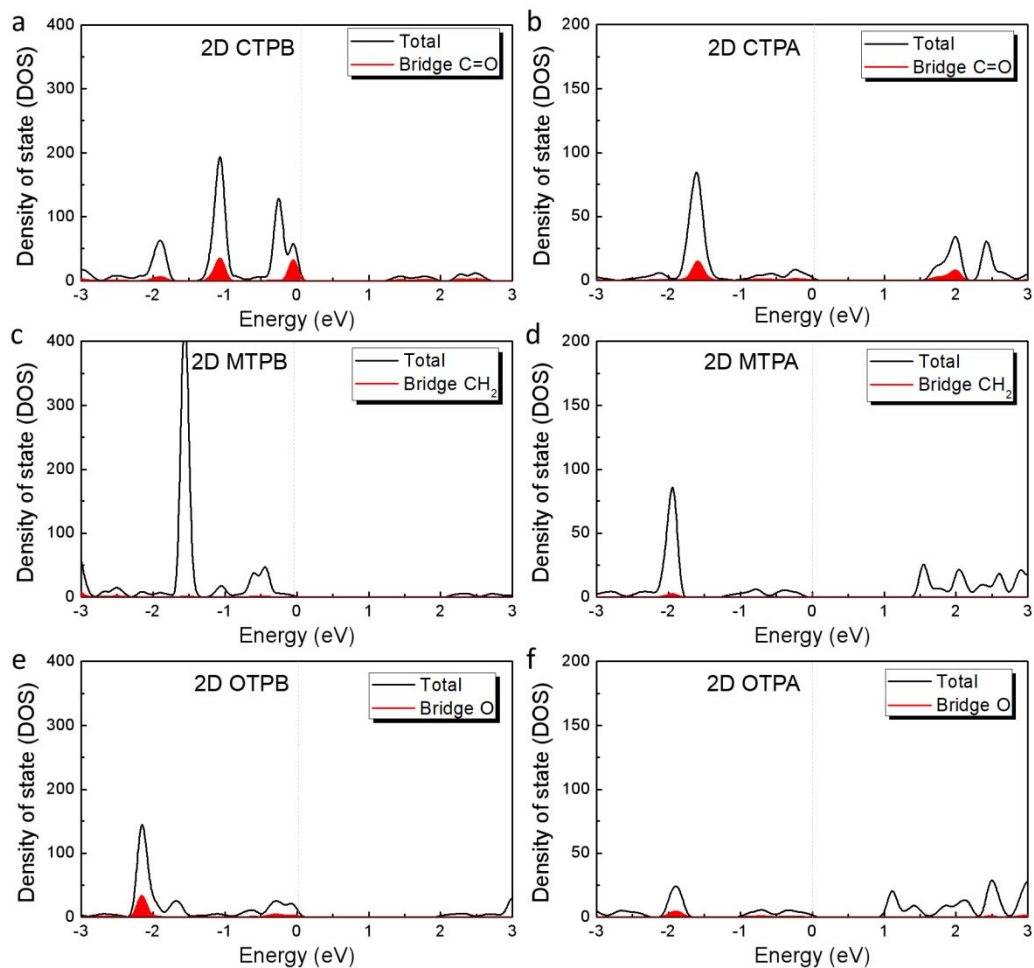


Figure S8. Density of state (DOS). (a-f) partial density of state (PDOS) contribution of the bridge group to the total DOS of **kgm** HT(N/B)-polymers calculated at the PBE level.

References

- (1) te Velde, G.; Bickelhaupt, F. M.; Baerends, E. J.; Fonseca Guerra, C.; van Gisbergen, S. J. A.; Snijders, J. G.; Ziegler, T. Chemistry with ADF. *J. Comput. Chem.* **2001**, *22*, 931-967.
- (2) Izmaylov, A. F.; Scuseria, G. E. Why are time-dependent density functional theory excitations in solids equal to band structure energy gaps for semilocal functionals, and how does nonlocal Hartree–Fock-type exchange introduce excitonic effects? *J. Chem. Phys.* **2008**, *129*, 034101.
- (3) Kronik, L.; Neaton, J. B. Excited-state properties of molecular solids from first principles. *Annu. Rev. Phys. Chem.* **2016**, *67*, 587–616.

-
- (4) Gonze, X.; Lee, C. Dynamical matrices, Born effective charges, dielectric permittivity tensors, and interatomic force constants from density-functional perturbation theory. *Phys. Rev. B: Condens. Matter Mater. Phys.* **1997**, *55*, 10355–10368.
 - (5) Togo, A.; Oba, F.; Tanaka, I. First-principles calculations of the ferroelastic transition between rutile-type and CaCl₂-type SiO₂ at high pressures. *Phys. Rev. B: Condens. Matter Mater. Phys.* **2008**, *78*, 134106.
 - (6) Bardeen, J.; Shockley, W. Deformation potentials and mobilities in non-polar crystals. *Phys. Rev.* **1950**, *80*, 72.
 - (7) Cai, Y.; Zhang, G.; Zhang, Y. W. Polarity-reversed robust carrier mobility in monolayer MoS₂ nanoribbons. *J. Am. Chem. Soc.* **2014**, *136*, 6269–6275.
 - (8) Qiao, J.; Kong, X.; Hu, Z. X.; Yang, F.; Ji, W. High-mobility transport anisotropy and linear dichroism in few-layer black phosphorus. *Nat. Commun.* **2014**, *5*, 4475.
 - (9) Long, M.; Tang, L.; Wang, D.; Li, Y.; Shuai, Z. Electronic structure and carrier mobility in graphdiyne sheet and nanoribbons: theoretical predictions. *ACS Nano*, **2011**, *5*, 2593–2600.
 - (10) Price, P. J. Two-dimensional electron transport in semiconductor layers. I. Phonon scattering. *Ann. Phys.* **1981**, *133*, 217.